

Large acceptance of non-collinear phase-matching second harmonic generation on the surface of an anomalous-like bulk dispersion medium

Xiaojing Wang,^{1,2} Huaijin Ren,^{1,2} Ning An,^{1,2} Xiaohui Zhao,^{1,2}
Yuanlin Zheng,^{1,2} and Xianfeng Chen^{1,2,*}

¹ Department of Physics and Astronomy, Shanghai Jiao Tong University, 800 Dongchuan Road, Shanghai 200240, China

² Key Laboratory for Laser plasmas (Ministry of Education), Shanghai Jiao Tong University, 800 Dongchuan Road, Shanghai 200240, China

*xfchen@sjtu.edu.cn

Abstract: We investigate several bandwidths of non-collinear phase-matching second harmonic generation, which is generated by sum-frequency of the incident and reflected wave on the inner surface of a z-cut 5%/mol $MgO : LiNbO_3$ crystal. The bandwidths of angle, temperature and wavelength in this configuration are measured to be about 0.51° , 4.1°C and 6 nm, respectively. The large acceptance of non-collinear phase-matching second harmonic generated on the surface shows attractive potential in the application of wavelength conversion.

© 2014 Optical Society of America

OCIS codes: (190.0190) Nonlinear optics; (240.0240) Optics at surfaces; (140.3515) Lasers, frequency doubled.

References and links

1. R. W. Boyd, *Nonlinear Optics* (Academic, San Diego, Calif., 1992).
2. J. Armstrong, N. Bloembergen, J. Ducuing, and P. Pershan, "Interactions between light waves in a nonlinear dielectric," *Phys. Rev.* **127**, 1918 (1962).
3. X. Deng and X. Chen, "Domain wall characterization in ferroelectrics by using localized nonlinearities," *Opt. Express* **18**(15), 15597–15602 (2010).
4. A. Fragemann, V. Pasiskevicius, and F. Laurell, "Second-order nonlinearities in the domain walls of periodically poled KTiOPO 4," *Appl. Phys. Lett.* **85**, 375–377 (2004).
5. H. Ren, X. Deng, Y. Zheng, N. An, and X. Chen, "Nonlinear Cherenkov radiation in an anomalous dispersive medium," *Phys. Rev. Lett.* **108**, 223901 (2012).
6. H. Huang, C.P. Huang, C. Zhang, D. Zhu, X.H. Hong, J. Lu, J. Jiang, Q.J. Wang, and Y.Y. Zhu, "Second-harmonic generation in a periodically poled congruent LiTaO₃ sample with phase-tuned nonlinear Cherenkov radiation," *Appl. Phys. Lett.* **100**, 022905 (2012).
7. Y. Sheng, V. Roppo, Q. Kong, K. Kalinowski, Q. Wang, C. Cojocar, J. Trull, and W. Krolikowski, "Tailoring Čerenkov second-harmonic generation in bulk nonlinear photonic crystal," *Opt. Lett.* **36**, 2593–2595 (2011).
8. N. An, H. Ren, Y. Zheng, X. Deng, and X. Chen, "Cherenkov high-order harmonic generation by multistep cascading in χ^2 nonlinear photonic crystal," *Appl. Phys. Lett.* **100**, 221103 (2012).
9. P. Xu, S. Ji, S. Zhu, X. Yu, J. Sun, H. Wang, J. He, Y. Zhu, and N. Ming, "Conical Second Harmonic Generation in a Two-Dimensional χ^2 Photonic Crystal: A Hexagonally Poled LiTaO₃ Crystal," *Phys. Rev. Lett.* **93**, 133904 (2004).
10. Z. Xie, G. Zhao, P. Xu, Z. Gao, and S. Zhu, "Study of optical elastic scattering in a quasiperiodically poled LiTaO₃ crystal," *J. Appl. Phys.* **101**, 056104 (2007).
11. K. Bastwöste, U. Sander, and M. Imlau, "Conical light scattering in strontium barium niobate crystals related to an intrinsic composition inhomogeneity," *Phys.: Condens. Matter* **19**, 156225 (2007).
12. Murib, Mohammed Sharif and Yüce, Emre and Gürlü, Oğuzhan and Serpengüzel, "Polarization behavior of elastic scattering from a silicon microsphere coupled to an optical fiber," *Photon. Res.* **2**(2), 45–50 (2014).

13. N. An, Y. Zheng, H. Ren, X. Deng, and X. Chen, "Conical second harmonic generation in one-dimension non-linear photonic crystal," *Appl. Phys. Lett.* **102**, 201112 (2013).
14. H. Ren, X. Deng, Y. Zheng, N. An, and X. Chen, "Surface phase-matched harmonic enhancement in a bulk anomalous dispersion medium," *Appl. Phys. Lett.* **103**, 021110 (2013).
15. H. Ren, X. Deng, Y. Zheng, N. An, and X. Chen, "Enhanced nonlinear Cherenkov radiation on the crystal boundary," *Opt. Lett.* **38**, 1993–1995 (2013).
16. A. Zembrod, H. Puell, and J. Giordmaine, "Surface radiation from non-linear optical polarisation," *Opt. Quantum. Electron.* **1**, 64–66 (1969).
17. A. Aleksandrovsky, A. Vyunishev, A. Zaitsev, A. Ikonnikov, and G. Pospelov, "Ultrashort pulses characterization by nonlinear diffraction from virtual beam," *Appl. Phys. Lett.* **98**, 061104 (2011).
18. O. Gayer, Z. Sacks, E. Galun, and A. Arie, "Temperature and wavelength dependent refractive index equations for MgO-doped congruent and stoichiometric LiNbO₃," *Appl. Phys. B* **91**, 343–348 (2008).
19. Y. Chen, K. Su, T. Lu, and K.-F. Huang, "Manifestation of weak localization and long-range correlation in disordered wave functions from conical second harmonic generation," *Phys. Rev. Lett.* **96**, 033905 (2006).

1. Introduction

Second-harmonic generation (SHG) is one of the most appealing parametric processes in non-linear optics and the conversion efficiency of SHG depends crucially on the phase-matching relations between the fundamental and SHG. Conventionally, these conditions can be achieved by taking advantages of two methods: birefringence phase matching (BPM) [1] which needs precisely control the direction of interactive waves and temperature of the crystal to satisfy phase-matching condition, quasi-phase-matching (QPM) [2–4] which involves a periodic modulation of second-order nonlinearity coefficient to supply the reciprocal vector $G_m = 2\pi m/\Lambda$ (Λ , m) to compensate for the mismatched phase. Besides, there are some other types of phase-matching approaches. For example, nonlinear Cherenkov radiation [5–8] with only the longitudinal phase-matching condition being satisfied, and conical second harmonic wave which is generated by the incident wave and its own scattering wave in a χ^2 photonic crystal [9–13]. Recent, we propose a surface complete phase-matching method [14–16] which utilizes sum-frequency wave generated by incident and reflected wave on the boundary of nonlinear crystal through non-collinear phase-matching process in anomalous-dispersion-like environment [17].

The surface complete phase-matching type has its own advantages of relative high conversion efficiency and easy realization. In our previous research [14], we have already observed the phenomenon, analyzed the triangle phase-matching relationship, and measured the conversion efficiency which is up to 15.74% of this surface complete phase-matching SHG. In order to investigate potential applications of this kind of configuration, the knowledge of bandwidths of angle, temperature and wavelength is necessary. In this letter, we focus our attention on these three parametric bandwidths of this efficient surface phase-matching method. By utilizing the measured bandwidths, we can estimate the interaction length of this phase-matching SHG and give useful information to estimate the enhancement of nonlinear coefficients in the future research work.

In the experiment, the crystal is a z-cut 5%/mol $MgO : LiNbO_3$ crystal of the size $3 \times 10 \times 2 \text{ mm}^3$, with all the six surfaces polished. The working temperature is 25°C. Through calculating of the Sellmeier equation [18], the refractive index of extraordinary-polarized SHG 532 nm is smaller than that of ordinary-polarized fundamental wave 1064 nm. This condition can simulate anomalous dispersion environment [5, 18] when the phase-matching type is o-o-e. The x-z plane of the crystal is placed on the rotating stage, the center wavelength we use as the fundamental wave is 1064 nm with 4 ns pulse width and 20 Hz repetition rate. The vertically-polarized (ordinary-polarized) fundamental wave is loosely focused right onto the x-y plane of the sample through a 250 mm focal length lens. The output horizontally-polarized (extraordinary-polarized) SHG is then projected onto a screen which is set 5 cm away from the sample. As shown in Fig. 1(a), when the ordinary-polarized fundamental wave is projected into

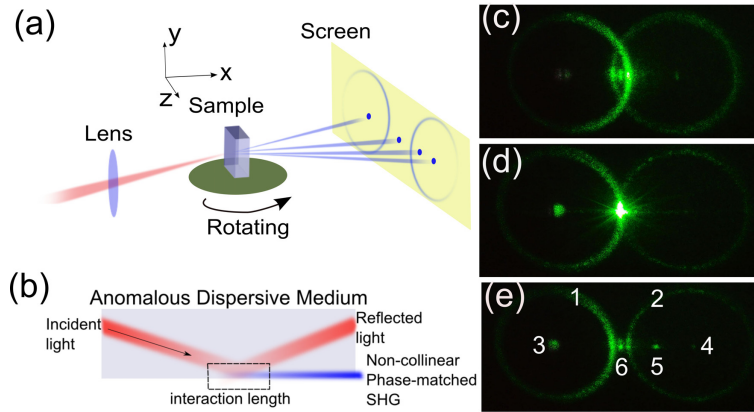


Fig. 1. (a) Schematic of the experiment setup. (b) Scheme of surface complete phase-matching SHG under anomalous dispersion condition. (c)-(e) The photographs exhibited on the screen when the incident fundamental wave is projected into the x-y plane of the crystal with different angles.

the x-y plane of the crystal with the angle larger than the requirement of total reflection, the experimental phenomenon exhibited on the screen is very affluent. The process of the intensity of the centric non-collinear SHG with the variation of the angle is shown in Figs. 1(c)–1(e). In Fig. 1(e) there are two conical SHG beams which distribute in an axial symmetry type 1 and 2, and three symmetrical distributed SHG spots 3,4,6 and one Cherenkov radiation spot 5 which is emitted from the crystal side. When the crystal on the stage is rotated to a special angle with the incident light, the intensity of centric SHG 6 is significantly enhanced. At the same time two conical SHG are tangent with each other, and NCR disappears, as shown in Fig. 1(d).

The physical mechanism of this phenomenon can be interpreted by four categories of phase-matching: (1) The two conical SHG beams are due to non-collinear phase-matching in which the incident and reflected light interacts with their own scattering waves to act as the fundamental waves, respectively. Scattering light can act as an additional fundamental wave in bulk crystal [5, 10] and scattering sources are due to imperfections on surface and impurity ions inside the crystal [13, 16, 19]. This triangular phase-matching relationship is analyzed in our previous research [14, 15]. (2) The bilateral SHG spots 3,4 of three symmetrically distributed SHG spots are the outcome of the collinear phase-mismatched SHG of the incident and reflected wave, respectively. (3) The centric SHG spot 6 is the outcome of non-collinear SHG generated by the sum-frequency polarization wave of the incident and reflected wave. (4) The nonlinear Cherenkov radiation (NCR) spot 5 is due to that the incident and reflected wave stimulate a sum-frequency polarization wave which emits the NCR when the wave vector of the polarization wave is smaller than that of the second harmonic wave [14].

In our experiment, the research focus is the bandwidth of the centric non-collinear phase-matching SHG spot 6. The phase-mismatched vector $\Delta\vec{k}$ of the centric SHG is $\vec{k}_2 - 2\vec{k}_1$. \vec{k}_1 , \vec{k}_2 is the wave vector of the fundamental and second harmonic wave, respectively. The scalar quantity of this phase-mismatched factor is

$$\Delta k = 4\pi(n_{2e} - n_{1o} \cos \theta) / \lambda_1 \quad (1)$$

where θ is the internal angle between incident wave and the x-axis, λ_1 is the wavelength of the fundamental wave, n_{2e} , n_{1o} is the index of SH and fundamental wave. When $\Delta k < 0$, two conical SH beams intersect with each other (Fig. 2(b)-a1). When $\Delta k = 0$, two conical SH beams are tangent with each other (Fig. 2(b)-a2). In this condition, the intensity of centric SH is en-

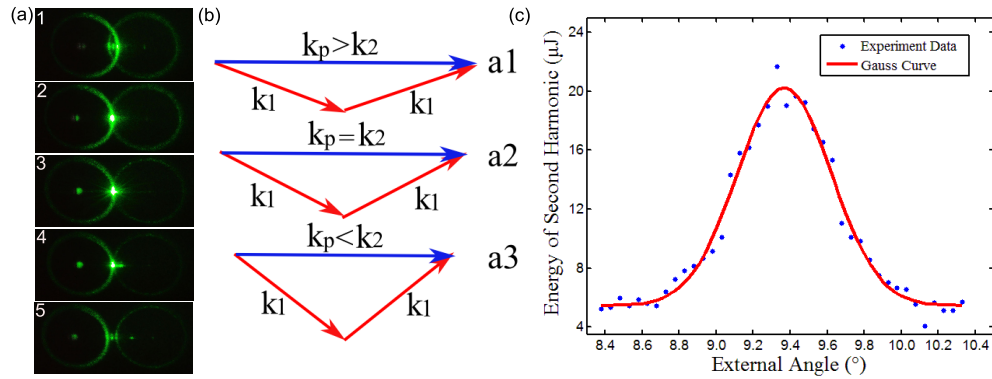


Fig. 2. (a) The changing process of the intensity of the centric non-collinear SHG spot under different incident angles with the x axis of the crystal. (b) Diagrams of phase-matching and phase-mismatching of the centric non-collinear SHG spot. (c) Measured power of the non-collinear phase-matching SHG as a function of external incident angles.

hanced significantly because the triangle phase-matching condition is completely satisfied for the centric SHG. The scattering light is replaced by the incident or reflected light which is coincidentally parallel to the scattering light in corresponding direction [14]. When $\Delta k > 0$, two conical SH beams separate with each other (Fig. 2(b)-a3). In this case, NCR appears. From the derivation of nonlinear wave coupling equation [1], the intensity of the second harmonic wave I_2 is proportional to $I_2 \sim d_{eff}^2 I_1^2 l^2 [\sin(\Delta kl/2)/(\Delta kl/2)]^2$, where l is the interaction length as is shown in Fig. 1(b), d_{eff} is the effective nonlinear coefficient, and Δk is the phase-mismatched factor. When Δk goes to zero, this situation corresponds to the complete phase-matching condition. Under this circumstance $[\sin(\Delta kl/2)/(\Delta kl/2)]^2 = 1$, I_2 arrives the maximum. The second harmonic conversion efficiency we measured in this situation is up to 15.74% when the average power of the second harmonic wave and the incident wave is approximate 0.885 mw and 5.22 mw, respectively. According to Eq. (1) and the Sellmeier equation [18], the phase-mismatch vector is relative to θ , T , λ and the information of bandwidths of these three parameters is very important for its practical applications. In the following parts, we investigate the bandwidths of the angle, temperature and wavelength of this surface phase-matching method.

2. Experiment

To investigate the bandwidth of angle, the temperature of the crystal is set at 20°C, and vertically polarized (ordinary-polarized) 1064 nm light is used to illuminate the x-y plane of the crystal. The energy of the emitted non-collinear horizontally polarization (extraordinary-polarized) SHG is measured. It is convenient for us to adjust the angle θ between the incident light and the x-axis of the crystal. The changed process of the intensity of centric non-collinear SHG under different incident angles with the x axis of the crystal is shown in Fig. 2(a). Theoretically, as analyzed before, θ is directly associated with the quantity of Δk . By rotating the x-z plane of the crystal, we could change θ , so consequently change the quantity of Δk which is directly related to the variation of the intensity of centric SHG. The measured maximum power of the centric SHG is 0.885 mw when the power of the fundamental wave is about 5.22 mw. The angle bandwidth measured is approximate 0.51° which is shown in Fig. 2(c).

Research on the temperature bandwidth is devised by placing the y-z plane of the crystal in two heating and cooling plates and fixing the external incident light at 8.62° which is exactly the complete phase-matching external incident angle with the x-axis at the temperature

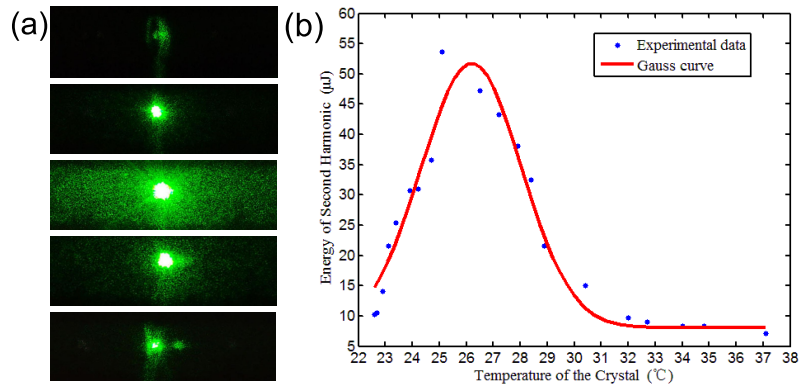


Fig. 3. (a) The changed process of the intensity of the centric non-collinear SHG under different temperature of the crystal. (b) Measured power of the non-collinear phase-matching SHG as a function of temperature of the crystal.

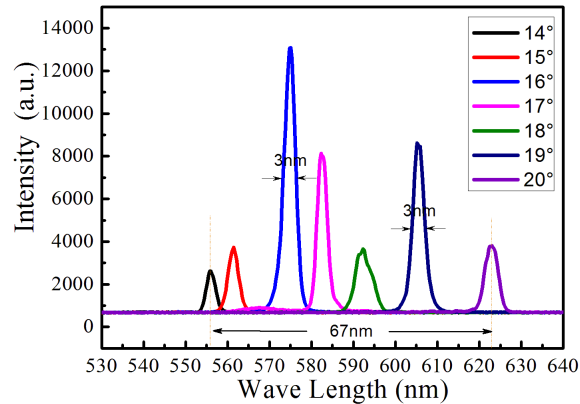


Fig. 4. The spectrum of SHG corresponds to different center wavelength of fundamental wave.

of 25°C. The heating and cooling plates could help change the temperature of the crystal. If the temperature of crystal is changed, n_{1o} , n_{2e} will change subsequently because the dependence of refractive index on temperature. This can cause the deviation of Δk from 0 through calculation of Eq. (1), and finally change the intensity of the centric SHG beam. Through using the horizontally polarized (ordinary-polarized) 1064nm as fundamental wave to illuminate the x-y plane of the crystal at the same incident angle, and measuring the intensity of the emitted SHG, the bandwidth of temperature can be researched. The changed process of the intensity of the centric non-collinear SHG beam is shown in Fig. 3(a). In our experiment the temperature bandwidth of the crystal measured is approximate 4.1°C, as shown in Fig. 3(b).

In the measurement of the wavelength bandwidth we use the optical parametric amplifier(TOPAS, Coherent, Inc) femtosecond laser system which can supply tunable wavelength from 280 nm to near 2600 nm to supply the fundamental wave. The temperature of the crystal is set at 18°C. The laser beam has a nearly Gaussian profile with a pulse width of 80 fs, and a repetition rate of 1000 Hz. The laser beam is loosely focused into the crystal by a 250 mm focal

lens. In our experiment, the x-z plane of the crystal is placed on a rotation stage, the crystal is illuminated along the x-y plane with the vertically polarized (ordinary-polarized) laser beam at the centric wavelength of 1190 nm with the bandwidth about 75 nm. In order to satisfy phase-matching requirement, we can fix the external angle from 14° to 20° , respectively. Each of these angles corresponds to one certain external phase-matching angle of centric SHG for different incident wave (centric wavelength 1112 nm, 1122 nm, 1150 nm, 1164 nm, 1184 nm, 1210 nm 1246 nm). So we can obtain different spectral components of the pump pulse corresponding to these different centric non-collinear phase-matching SHG as shown in Fig. 4. Measuring the bandwidth of SH wave 575 nm, we can get the bandwidth of SHG is approximate 3 nm as shown in Fig. 4. In order to satisfy $2k_{1o}\cos\theta = k_{2e}$, one incident angle only corresponds to one certain wavelength. The mechanism of this type of phase-matching is narrowband, which is the same as the BPM and QPM technique [1,2]. Due to the quadratic relationship between the SHG and the fundamental wave intensity in the frequency conversion, the wavelength bandwidth of fundamental wave is about 6 nm.

The statistic we obtain from three bandwidth experiments illustrates that the surface complete phase-matching SHG has a large acceptance bandwidth of angle, temperature, and wavelength. A single total reflection on the surface could provide high conversion efficiency which is up to 15.74% with a short interaction volume. We believe that a higher conversion efficiency could be realized through multi-pass reflection. These advantages provide this type of phase-matching SHG more tolerance to be generated, and so make it have more extensive application in optical microscopy, surface detection, optical manipulation, optical measurement, and other aspects.

3. Conclusion

In conclusion, we demonstrate the phenomenon of conical SHG, collinear phase-mismatched SHG, non-collinear phase-matching SHG and NCR beam generated on the surface of an anomalous-like bulk dispersion medium, and analyze their physical mechanism. The measured the angle bandwidth, temperature bandwidth, and wavelength bandwidth of the non-collinear phase-matching SHG is 0.51° , 4.1°C and 6 nm, respectively. All of these parameters are associated with the quantity of phase-mismatched. In the future research we will propose one method to estimate the interaction length of this surface non-collinear phase-matching by utilizing the measured results, and finally estimate the corresponding enhancement of nonlinear coefficient on the surface.

Acknowledgments

This work was supported in part by the National Basic Research Program 973 of China under Grant No. 2011CB808101, the National Natural Science Foundation of China under Grant Nos. 61125503, 61235009, and 61205110, the Foundation for Development of Science and Technology of Shanghai under Grant No. 13JC1408300, and in part by the Innovative Foundation of Laser Fusion Research Center.